Available online at www.sciencedirect.com
ScienceDirect
Polymer 49 (2008) 1761–1769
polymer
www.elsevier.com/locate/polymer

Synthesis of thermoresponsive poly(*N*-isopropylmethacrylamide) and poly(acrylic acid) block copolymers via post-functionalization of poly(*N*-methacryloxysuccinimide)

Jeremy M. Rathfon, Gregory N. Tew*

Department of Polymer Science and Engineering, University of Massachusetts, 120 Governors Drive, Amherst, MA 01003, United States

Received 17 December 2007; received in revised form 24 January 2008; accepted 26 January 2008
Available online 7 February 2008

Abstract

Polymers exhibiting a thermoresponsive, lower critical solution temperature (LCST) phase transition have proven to be useful for many applications as ''smart'' or ''intelligent'' materials. A series of poly(*N*-isopropylmethacrylamide) (PNIPMAM) polymer, poly(*N*-isopropylmethacrylamide)-*b*-poly(acrylic acid) (PNIPMAM-*b*-PAA) diblock, and poly(acrylic acid)-*b*-poly(*N*-isopropylmethacrylamide)-*b*-poly(acrylic acid) (PAA-*b*-PNIPMAM-*b*-AA) triblock copolymer samples were synthesized via ATRP. A facile post-functionalization route was developed that uses an activated ester functionality to convert poly(*N*-methacryloxysuccinimide) (PMASI) blocks to LCST capable polyacrylamide, while poly(*t*-butyl acrylate) (P*t*BA) blocks were converted to water-soluble poly(acrylic acid) (PAA). The post-functionalization was monitored via ^{1}H NMR and ATR-FTIR. The aqueous solution properties were explored and the PNIPMAM polymers were shown to have a LCST phase transition varying from 35 to 60 °C. The ability to synthesize block copolymers that are thermoresponsive and water-soluble will be of great benefit for broader applications in drug delivery, bioengineering, and nanotechnology.

Keywords: Atom transfer radical polymerization (ATRP); Lower critical solution temperature (LCST); Thermoresponsive polymers

1. Introduction

Many polymers show a reversible phase transition in response to an increase in temperature, known as a lower critical solution temperature (LCST). This LCST transition has been studied for many polyacrylamides including poly(*N*-isopropylacrylamide) (PNIPAM) and poly(*N*-isopropylmethacrylamide) (PNIPMAM) [1,2]. Recently, there has been increasing interest in polymers exhibiting LCST properties for the design of ''intelligent'' or ''smart'' materials [3–17]. The thermoresponsive nature of these polymers has led to applications in drug delivery [13–16], bioengineering [5,8,9,11], nanotechnology [6,7,10,12,17], and a promising future for applications in the areas of biosensors and membranes.

The LCST transition is driven by an increase in entropy upon heating, due to the loss of both the hydration of the hydrophilic amide group and the hydrophobic interactions of the alkyl pendant group, where entropy of the pendant group outweighs the enthalpic contribution [18]. Typically the cloud point of a dilute polymer solution is reported as an indicator of the polymer sample's thermoresponsive nature, rather than the LCST minimum of a polymer/water phase diagram [19]. The cloud point ($T_{50\%}$) is defined as the temperature at which normalized transmittance is reduced to 50% during the phase transition. For polyacrylamides, the cloud point has been shown to be dependent on concentration [20–22], end group composition [19,23,24], and molecular weight (MW) [2,21,22,25–34]. The majority of these studies used conventionally polymerized samples without well-defined polymers of low polydispersity (PDI), which prevented precise examination of the LCST transition. These previous studies showed that the well-controlled synthesis of LCST polymers,

* Corresponding author.
E-mail address: tew@mail.pse.umass.edu (G.N. Tew).

0032-3861/$ - see front matter © 2008 Elsevier Ltd. All rights reserved.
doi:10.1016/j.polymer.2008.01.071

to generate polymers with narrow PDI, is essential to provide a better understanding of the phase transition.

The synthesis of polyacrylamides has been approached using many techniques. The most commonly used polymerization method is controlled free radical polymerization (CFRP) including atom transfer radical polymerization (ATRP) [18,19,23,35–39], reversible addition fragmentation chain-transfer (RAFT) polymerization [24,40–44], and nitroxide mediated polymerization (NMP) [45,46]. In most cases, these polymerization techniques prove to be difficult for acrylamides, yielding higher polydispersities, low MWs, or requiring special reaction conditions [18,19,35–46]. For the ATRP of polyacrylamides, control over polydispersity is difficult due to several reasons: deactivation of the copper catalyst due to complexation with the amide group, a cyclization reaction of the bromine end with the penultimate amide nitrogen, and an inadequate redox potential of the catalysts causing increased radical concentration and thus biradical termination. All of the above factors result in difficult to control polymerizations for the ATRP of acrylamides and thus polydispersity index (PDI) values ranging from approximately 1.1 to 3 occurred [35,37–39]. Good control for the ATRP of PNIPAM homopolymers has been achieved, using more dynamic catalyst/initiator pairs and various polar solvents tuned specifically for the conditions [18,19,35].

This paper discusses the synthesis of PNIPMAM via a post-functionalization route. An activated ester, *N*-methacryloxysuccinimide (MASI), was polymerized via ATRP. MASI has been shown to polymerize in a controlled ''living'' fashion via ATRP and is able to initiate a second monomer [47]. MASI has been used previously by our group to synthesize well-controlled block copolymers that can later be functionalized with various groups to achieve polymers with different properties [48,49]. Here, poly(*N*-methacryloxysuccinimide) (PMASI) homopolymer and block copolymers were functionalized to create PNIPMAM samples with thermoresponsive solution properties. The controlled synthesis of polymer and block copolymer samples of PNIPMAM with low polydispersity will be discussed in this paper. The aqueous solution properties of these polymers are explored to show response to temperature change, probing their LCST nature.

2. Experimental

2.1. Materials

All chemical reagents were purchased from Aldrich, Alfa Aesar, Fisher, Cambridge Isotopes Aldrich, or Acros Organics and used without further purification unless otherwise stated. To remove methyl ether hydroquinone (MEHQ) inhibitor, *t*-butylacrylate (*t*BA) was washed three times with an aqueous solution of 5 wt% NaOH, followed by washing three times with distilled water. *t*BA was then dried over $MgSO_4$, followed by CaH_2, vacuum distilled, and then stored under nitrogen at −20 °C. Water used for LCST studies was purified using a Millipore Milli-Q UF Plus system with a QPAK 1 column. All syringe injections for water and air sensitive reactions were made using a syringe purged with nitrogen gas three times, immediately prior to use.

2.2. Measurements

^{1}H NMR (400 MHz) and ^{13}C NMR (100 MHz) spectra were obtained in DMSO-d_6 using a Bruker Avance NMR spectrometer. Gel permeation chromatography (GPC) was performed in 0.05 M LiBr/dimethylformamide (DMF) solution at 50 °C (1.0 mL/min) with a Polymer Labs GPC 50 using two Polymer Labs Resipore® columns (3 μm, 300 mm × 7.5 mm) and calibrated with narrow-MW, linear poly(methyl methacrylate) standards. UV–vis spectra were obtained with a Perkin–Elmer Lambda 2 series spectrophotometer with PECSS software. Attenuated total reflectance-Fourier transform infrared (ATR-FTIR) spectroscopy was obtained using a Perkin–Elmer Spectrum One spectrometer with a Universal Diamond ATR sampling accessory.

2.3. Synthesis of the MASI monomer

N-Hydroxysuccinimide (50.0 g, 434 mmol), triethylamine (72.7 mL, 521 mmol), and dichloromethane (DCM) (500 mL) were added to a 1 L round-bottomed flask (RBF) equipped with a stir-bar. The flask was sealed and placed in an ice-bath at 0 °C. The solution was vigorously stirred while methacryloyl chloride (46.7 mL, 478 mmol) was added drop-wise. The reaction was stirred for 2 h under nitrogen slowly coming to room temperature. DCM (200 mL) was added to the reaction mixture and the organic layer was washed with 400 mL aqueous solution of 1 wt% $NaHCO_3$ and then washed twice with distilled water. The organic layer was concentrated under reduced pressure, then 300 mL 1:1 ethyl acetate/hexane mixture was added. The solution was allowed to crystallize at 4 °C overnight. The product, MASI monomer, was isolated via filtration, washed with hexane, dried under vacuum, then stored at −20 °C until use. Yield was ~70%. The MASI monomer was found to be ~95% pure via ^{1}H NMR. ^{1}H NMR (DMSO-d_6, ppm) $\delta = 6.3$ (s, H, $H_2C{=}C$), 6.1 (s, H, $H_2C{=}C$), 2.84 (s, 4H, MASI H), 2.00 (s, 3H, CH_3).

2.4. Synthesis of PNIPMAM polymers

For a typical polymerization, MASI (5.00 g, 27.3 mmol) and copper(I) bromide (CuBr) (89.1 mg, 0.621 mmol) were added to a dry 100 mL RBF equipped with a stir-bar. The flask was sealed and purged with dry nitrogen gas, passed through a drierite column. *N*,*N*,*N*′,*N*″,*N*″-pentamethyldiethylenetriamine (PMDETA) (130 μL, 0.621 mmol) and ethyl 2-bromoisobutyrate (EBIB) (90.2 μL, 0.621 mmol) were added to separate sealed vials and purged with dry nitrogen gas, then 2 mL of anhydrous anisole was added to each vial and bubbled with nitrogen. Anhydrous anisole (36 mL) was added to the RBF and the solution was bubbled with nitrogen. After 15 min, the PMDETA solution was added to the RBF via syringe and the reaction mixture was stirred for 20 min at

room temperature to allow catalyst formation, indicated by a color change to blue. The EBIB solution was added to the RBF via syringe then the reaction mixture was placed in a 90 °C oil bath for 1 h. The reaction ratio was [MASI]:[EBIB]:[CuBr]:[PMDETA] = 44:1:1:1. The reaction mixture was rapidly quenched with liquid nitrogen, then concentrated under reduced pressure. The crude mixture was purified twice by dissolving in a minimum amount of DMSO, followed by precipitation into acetone. The final filtered product, PMASI, was dried under vacuum. The targeted conversion of ~60% was achieved. ^{1}H NMR (DMSO-d_6, ppm) $\delta = 2.79$ (s, 4H, MASI H), 1.4 (br s, 3H, CH_3), 1.4 (br s, 2H, CH_2). ^{13}C NMR (DMSO-d_6, ppm) $\delta = 172.8$, 170.2, 45.1, 40.4, 25.6, 25.3, 18.0. IR (solid, cm^{-1}) $\nu = 1808$, 1778, 1732 (MASI bands), 1660, 1063, 645.

PMASI was functionalized to form PNIPMAM by amidation via the activated ester functional group. In a RBF, PMASI was dissolved in minimal DMF, then the flask was sealed and purged with nitrogen gas. Isopropylamine (4 equiv. to MASI units) was added via a syringe, then the reaction was stirred at 60 °C for 24 h. The polymer, PNIPMAM, was precipitated into ether, filtered, and dried under vacuum. Yield was typically >95%. ^{1}H NMR (DMSO-d_6, ppm) $\delta = 7.2$ (s, 1H, NH ring-opened amide), 6.94 (br s, 1H, NH), 6.7 (s, 1H, O*NH*CO ring-opened amide), 3.79 (s, 1H, CH), 2.2 (t, 4H, CH_2 ring-opened amide), 1.74 (br s, 2H, CH_2), 1.0 (br s, 3H, CH_3), 1.01 (d, 6H, *i*-propyl CH_3). ^{13}C NMR (DMSO-d_6, ppm) $\delta = 173.8$, 170.5, 40.6, 30.9, 30.7, 22.5, 21.8. IR (solid, cm^{-1}) $\nu = 1708$ (ring-opened amide I stretch), 1630 (amide I stretch), 1529 (amide II stretch).

2.5. Synthesis of PNIPMAM-b-PAA and PAA-b-PNIPMAM-b-PAA block copolymers

Telechelic PMASI (Br−PMASI−Br) was prepared under the same reaction conditions previously described for the PNIPMAM polymers, except that dimethyl 2,6-dibromoheptanedioate (DBHD) (135 μL, 0.621 mmol) was used and the reaction time was 2 h. ATRP of *t*BA was carried out using the Br−PMASI−Br macroinitiator. For the synthesis of poly(acrylic acid)-*b*-poly(*N*-isopropylmethacrylamide)-*b*-poly(acrylic acid) (PAA-*b*-PNIPMAM-*b*-PAA) (**2**), Br−PMASI−Br (4.28 g, 0.766 mmol) and CuBr (220 mg, 1.53 mmol) were added to a dry 100 mL RBF equipped with a stir-bar. The flask was purged with dry nitrogen gas, then DMSO (18 mL) was added to the RBF. PMDETA (321 μL, 1.53 mmol) was added to a sealed vial and purged with nitrogen. Subsequently, DMSO (2 mL) was added to the vial containing PMDETA via a syringe, and the solution was bubbled with nitrogen. The reaction mixture was stirred to dissolve the macroinitiator, while being bubbled with nitrogen. PMDETA was added to the reaction mixture via syringe, and the solution was stirred for 20 min to allow catalyst formation, indicated by a color change to blue. The reaction mixture was brought to 90 °C before *t*BA monomer (8.97 mL, 61.2 mmol) was added via syringe. The reaction ratio was [*t*BA]:[Br−PMASI−Br]:[CuBr]:[PMDETA] = 80:1:2:2. The reaction was stirred at 90 °C for 6 h, then quenched with liquid nitrogen. The reaction mixture was dissolved in 400 mL acetone and passed through a short neutral alumina column to remove the catalyst. The solution was concentrated under reduced pressure, then precipitated into ether and filtered. The collected polymer, P*t*BA-*b*-PMASI-*b*-P*t*BA) (**1**), was dried under vacuum. Conversion was typically 60%. ^{1}H NMR (DMSO-d_6, ppm) $\delta = 2.77$ (s, 4H, MASI H), 1.4 (br s, 3H, CH_3), 1.4 (br s, 2H, CH_2), 1.35 (d, 9H, *t*-butyl CH_3). ^{13}C NMR (DMSO-d_6, ppm) $\delta = 172.8$, 170.2, 80.1, 45.1, 40.4, 27.6, 25.6, 25.3, 18.0. IR (solid, cm^{-1}) $\nu = 1808$, 1778, 1732 (MASI bands), 1660.

P*t*BA-*b*-PMASI-*b*-P*t*BA (**1**) was functionalized with isopropylamine to form P*t*BA-*b*-PNIPMAM-*b*-P*t*BA using the same procedure described for the conversion of PMASI to PNIPMAM. The *t*BA units of P*t*BA-*b*-PNIPMAM-*b*-P*t*BA were then deprotected with trifluoroacetic acid (TFA) to form PAA-*b*-PNIPMAM-*b*-PAA (**2**). P*t*BA-*b*-PNIPMAM-*b*-P*t*BA was added to a 50 mL RBF equipped with a stir-bar. The flask was sealed, purged with nitrogen gas, and placed in an ice-bath at 0 °C. TFA (50 equiv. to *t*BA units) was added via a syringe and the reaction was stirred for 2 days. The reaction mixture was concentrated under reduced pressure, then precipitated into ether. The polymer, PAA-*b*-PNIPMAM-*b*-PAA (**2**), was collected by filtration, then dried under vacuum. ^{1}H NMR (DMSO-d_6, ppm) $\delta = 12.1$ (br s, 1H, COOH), 7.2 (s, 1H, NH ring-opened amide), 6.94 (br s, 1H, NH), 6.7 (s, 1H, O*NH*CO ring-opened amide), 3.76 (s, 1H, CH amide), 2.2 (t, 4H, CH_2 ring-opened amide), 2.2 (br s, 1H, CH AA backbone), 1.75 (br s, 2H, CH_2 NIPMAM), 1.5 (br, 2H, CH_2 AA), 1.0 (br s, 3H, CH_3), 0.99 (d, 6H, *i*-propyl CH_3). ^{13}C NMR (DMSO-d_6, ppm) $\delta = 175.9$, 173.8, 170.5, 40.6, 30.9, 30.7, 22.5, 21.8. IR (solid, cm^{-1}) $\nu = 1715$ (CO band), 1708 (ring-opened amide I stretch), 1630 (amide I stretch), 1529 (amide II stretch).

The synthesis of PNIPMAM-*b*-PAA was carried out in the same manner as PAA-*b*-PNIPMAM-*b*-PAA (**2**), with hemi-telechelic PMASI−Br macroinitiator used in place of Br−PMASI−Br. The ATRP reaction ratio was [*t*BA]:[PMASI−Br]:[CuBr]:[PMDETA] = 80:1:1:1.

2.6. LCST measurements

Solutions for LCST measurements were prepared by dissolving 10 mg of polymer (PNIPMAM, PNIPMAM-*b*-PAA, or PAA-*b*-PNIPMAM-*b*-PAA (**2**)) into 3 mL of Milli-Q purified water (pH = 5.4) to yield 0.33 wt% solutions. The solutions were sonicated and left to dissolve overnight. Percent transmittance of the samples, at 500 nm, was measured using the UV−vis spectrophotometer while temperature was varied from 25 °C to 75 °C, at a rate of 1 °C/min in 5 °C increments. The instrument was auto-zeroed against pure Milli-Q purified water. Percent transmittance data were normalized ($T_{norm} = [(T - T_{min})/(T_{max} - T_{min})]$), then plotted as transmittance versus temperature. The drop in transmittance around the LCST transition was fitted as exponential decay. This fit was then used to calculate the cloud point ($T_{50\%}$), the temperature at 50% transmittance.

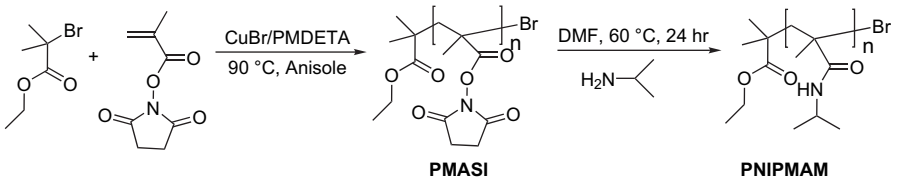

Scheme 1. Synthesis of PNIPMAM.

3. Results and discussion

3.1. PNIPMAM polymer synthesis

We reported previously the controlled homopolymerization of PMASI to MWs ranging from ~8 to 15 kDa [49]. For this study, PNIPMAM was synthesized via a novel post-functionalization approach of the activated ester, MASI, as shown in Scheme 1. The known problematic controlled polymerization of amides was avoided using this approach [18,19,35–46]. ATRP was used to synthesize a series of PMASI homopolymers with controlled MWs and polydispersity (Table 1). The samples of PMASI were then functionalized to form PNIPMAM through reaction of the activated ester functional group.

The conversion of PMASI to PNIPMAM was analyzed using ^{1}H NMR and ATR-FTIR. In the ^{1}H NMR (DMSO-d_6) spectra of the homopolymer, the MASI group has a distinct broad singlet at 2.79 ppm. The complete disappearance of this peak was seen in the spectrum of PNIPMAM after reaction, along with the simultaneous appearance of the N–H amide singlet, the methyne singlet, and the methyl doublet from the isopropylamide functional group as shown in Fig. 1. These spectral changes are consistent with the conversion of MASI to isopropylamide. In addition, the ATR-FTIR spectrum of PMASI has three distinct bands (1808, 1778, 1732 cm^{-1}) corresponding to the MASI functional group [49]. After reaction with isopropylamine, the ATR-FTIR spectrum shows that the characteristic MASI bands have been replaced with bands at 1630 and 1529 cm^{-1}, which are consistent with amide functionality (Fig. 2). Therefore, the post-functionalization of PMASI to PNIPMAM was confirmed to be greater than 99% by ^{1}H NMR and ATR-FTIR.

Putnam and Wong recently published a report detailing side reactions associated with PMASI precursor polymers [50]. The report outlines amines reacting with MASI to form the desired amides as well as a ring-opened amide and glutarimide side products (see Scheme 2). Putnam shows the reduction of these side products with increasing temperature between 25, 50, and 75 °C, while changing time or concentration had little effect on side product yield. Here, PMASI was reacted with isopropylamine at 60 °C. The ring-opened amide side product was found to be present via ^{1}H NMR, with peaks at 7.26 and 6.71 ppm corresponding to the two ring-opened amide protons, with a 1:1 ratio of integrated area (Fig. 1). The total ring-opened amide ratio was determined to be 23 mol% in the polymer samples. Putnam and Wong do not report the amido ester peak (e″ in Fig. 1) in the ring-opened structure due to overlapping benzyl peaks in their NMR spectra. The ring-opened amide side product may also be visible in the FTIR spectrum which would be consistent with a ring-opened amide I stretch at 1708 cm^{-1} (Fig. 2). In addition, this IR signal is weaker than the two other bands at 1529 and 1630 cm^{-1}, consistent with the ^{1}H NMR integration of ~23 mol % ring-opened amide. Interestingly, careful examination of the ^{1}H NMR spectrum shown in Fig. 1 does not show any evidence for the glutarimide side product. Specifically, Putnam and Wong reported a small downfield shoulder on the peak of the methylene adjacent to the amide nitrogen. The methylene shown in Fig. 1 at 3.79 ppm does not have a shoulder expected for the glutarimide. Neither of these side products have been observed by our group with the use of poly(*N*-succinimide *p*-vinylbenzoate) (PNSVB), a styrene based activated ester utilizing the same succinimide functionality [51].

Table 1
Data for the ATRP of MASI[a]

$[M]_0$:$[I]_0$:$[C]_0$	Time (h)	Conv[b] (%)	$M_{n,th}$[c] (kDa)	$M_{n,GPC}$[d] (kDa)	M_w/M_n[d]
40:1:1	1	86	6300	9600	1.19
44:1:1	1	58	4700	7000	1.11
87:1:1	1	37	5900	8400	1.19
87:1:1	2	50	7900	7500	1.17
100:1:1	1	52	9400	14,200	1.16
175:1:1	1	54	17,200	12,700	1.13
350:1:1	1	33	21,100	13,000	1.16
44:1:1[e]	2	64	5100	7400	1.14

[a] Experimental conditions: typically 5.00 g of MASI, 90 °C, $[M]_0 = 0.68$ M in anisole.
[b] Determined gravimetrically.
[c] $M_{n,th} = M_{MASI}[MASI]_0 conv/[EBIB]_0$.
[d] From GPC in 0.05 M LiBr/DMF.
[e] DBHD used as initiator.

4. Higher molecular weight PMASI

Previous work performed by our group optimized solvent choice, temperature, and reaction ratios for the successful polymerization of MASI [49]. The best reaction conditions were found to be polymerization in anisole at 90 °C. For the PMASI series shown in Table 1, the monomer to initiator ratio was increased to synthesize polymers with higher degrees of polymerization. Monomer concentration was varied from 0.32 M to 7.0 M (~50 wt% solvent) and 0.68 M concentration was found to give the best control over conversion and polydispersity. The resulting PMASI samples ranged from ~7 to 14 kDa

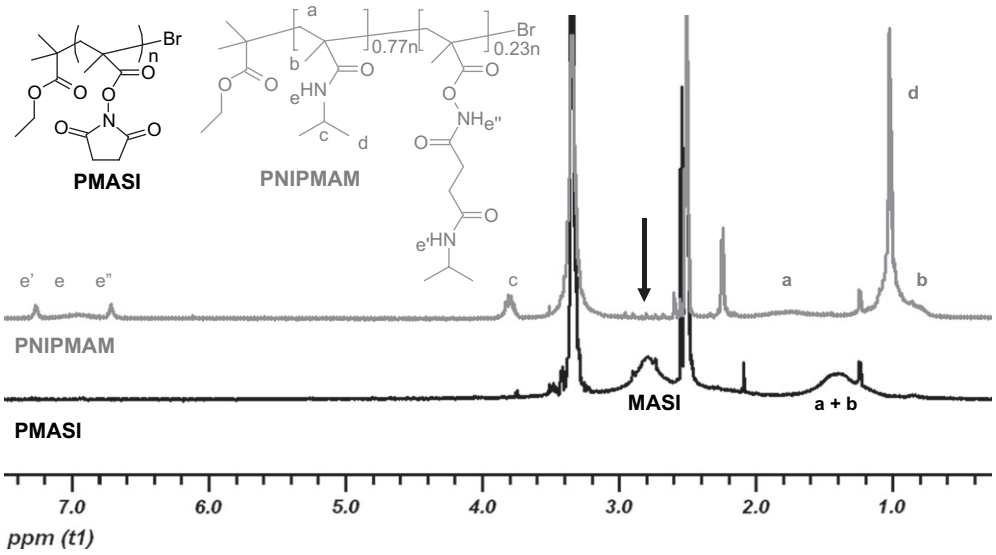

Fig. 1. ^{1}H NMR (DMSO-d_6) comparing PMASI (black) with PNIPMAM (gray).

with polydispersities of 1.11–1.19, illustrating control over MW and polydispersity.

Although control over MW and polydispersity was demonstrated with the ATRP of MASI monomer to form well-defined PMASI, then converted to PNIPMAM samples, higher conversion of larger MW PMASI targets was difficult to obtain. For the reaction of MASI with the molar ratio of $[M]_0$:$[I]_0$:$[C]_0 = 350$:1:1, a conversion of only 33% ($M_{n,GPC} = 13.0$ kDa) was obtained after 1 h (Table 1). Using the same reaction ratios, longer reaction times (up to 48 h) yielded similar conversions with approximately the same MW, but typically accompanied by higher PDI (>1.3). Lowering the monomer to initiator ratio (from $[M]_0$:$[I]_0$:$[C]_0 = 350$:1:1 to $[M]_0$:$[I]_0$:$[C]_0 = 175$:1:1 and $[M]_0$:$[I]_0$:$[C]_0 = 100$:1:1) yielded similar results where a MW threshold of approximately 14 kDa was achieved, regardless of reaction time. We speculate that the threshold of MW is due to aggregation of the polymer chains as they grow in size during polymerization [52]. The aggregation makes the chains less accessible to available monomer in solution and polydispersity increases due to the aggregation of chains and side reactions from this concentrated aggregate, while free chains continue to propagate in solution. Further work is required to elucidate the exact cause of the observed MW limit; however, it is known that anisole is not a good solvent for PMASI. This MW threshold of PMASI corresponds to approximately 9 kDa for functionalized PNIPMAM polymer.

Given the upper MW limit, a series of PNIPMAM polymers with low polydispersity indexes (1.13–1.23) and varying MWs (3.6–9.1 kDa) were synthesized (Table 2) via post-functionalization of the activated ester. The aqueous solution properties of these polymers were studied to examine the effects of MW and polydispersity on the LCST transition.

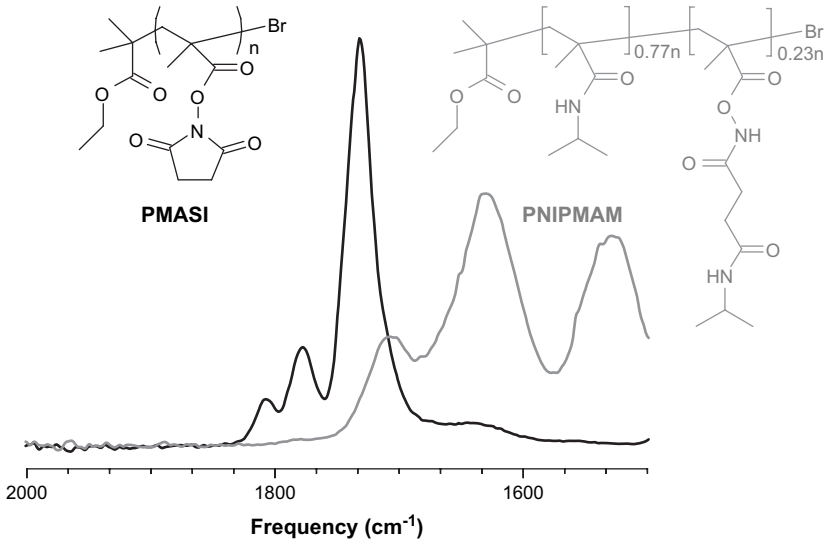

Fig. 2. FTIR overlay of PMASI (black) and PNIPMAM (gray).

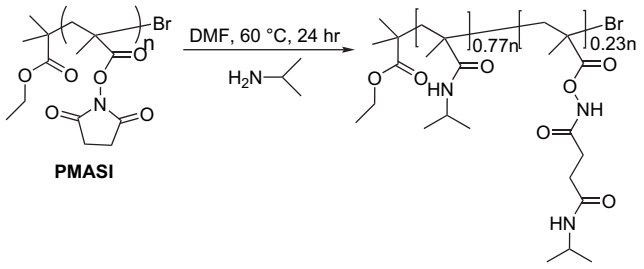

Scheme 2. Side reaction of PMASI.

Table 2
M_n and $T_{50\%}$ for the PNIPMAM polymer series

Calc. M_n (kDa)	PDI	$T_{50\%}$ (°C)
3.6	1.23	39.6 ± 0.9
4.2	1.17	47.8 ± 0.3
4.3	1.16	52.6 ± 0.2
6.7	1.18	47.6 ± 1.4
8.8	1.13	57.9[c]
9.1	1.16	58.3[c]
6.7[a]	1.25	45.6[c]
5.5[b]	1.24	38.8[c]

[a] Calc. M_n for PNIPMAM block of PNIPMAM-*b*-PAA.
[b] Calc. M_n for PNIPMAM block of PAA-*b*-PNIPMAM-*b*-PAA (**2**).
[c] Only single data point recorded.

4.1. PNIPMAM-b-PAA and PAA-b-PNIPMAM-b-PAA block copolymer synthesis

PNIPMAM-*b*-PAA and PAA-*b*-PNIPMAM-*b*-PAA (**2**) block copolymers were synthesized via the same post-functionalization approach as the PNIPMAM polymers (Scheme 3). Hemi-telechelic and telechelic brominated PMASI macroinitiators were synthesized using ATRP following the procedures outlined earlier. These macroinitiators were block extended with *t*BA monomer to form the corresponding diblock PMASI-*b*-P*t*BA and triblock P*t*BA-*b*-PMASI-*b*-P*t*BA (**1**) copolymers. Overlaid GPC traces of PMASI and P*t*BA-*b*-PMASI-*b*-P*t*BA (**1**) polymers show a clear shift in the MW, indicating good initiation of *t*BA from the PMASI macroinitiator (Fig. 3). The MASI segments were then post-functionalized with isopropylamine through reaction of the activated ester group to form PNIPMAM blocks. The *t*BA polymer segments were deprotected using TFA to form the PAA blocks.

The post-functionalization and deprotection of the resultant block copolymers were studied using ^{1}H NMR and ATR-FTIR. The substitution of MASI with the isopropylamide group was followed by monitoring the disappearance of MASI peaks and the emergence of the isopropylamide peaks in the ^{1}H NMR and ATR-FTIR spectra as discussed previously. No side reactions of *t*BA were seen during the post-functionalization reaction. For both diblock and triblock copolymers, the deprotection of *t*BA to AA was also followed. In the ^{1}H NMR (DMSO-d_6) spectra, *t*BA has a singlet at 1.35 ppm. The disappearance of this peak and the emergence of the AA carboxylic acid peak, a broad singlet at 12.15 ppm, supports the conversion of *t*BA to AA (Fig. 4). The FTIR spectra corresponding to this functionalization are complicated due to overlapping MASI and isopropylamide bands. However, high conversion of P*t*BA to PAA using this chemistry was proven in an earlier studies by our group, using an analogous polystyrene-*b*-poly(*t*-butyl acrylate) block copolymer [53] and a poly(*t*-butyl acrylate) homopolymer [54].

ATRP was used successfully to synthesize well-defined block copolymers PMASI-*b*-P*t*BA and P*t*BA-*b*-PMASI-*b*-P*t*BA (**1**). These polymers were post-functionalized to create PNIPMAM-*b*-PAA and PAA-*b*-PNIPMAM-*b*-PAA (**2**) block copolymers. Functionalization was shown to be nearly quantitative by following the reactions carefully via ^{1}H NMR and ATR-FTIR.

4.2. LCST study

In order to study the LCST behavior of these PNIPMAM polymers and block copolymers, samples were dissolved in Milli-Q water at 0.33 wt% and transmittance at 500 nm was measured while varying the temperature. The data collected from percent transmittance measurements were normalized and then plotted as transmittance versus temperature (Fig. 5A). The drop in transmittance at the LCST transition was fitted as an exponential decay and used to calculate the cloud point, $T_{50\%}$. (Fig. 5B) The square of the correlation coefficient (R^2) values were always greater than 98.5%, indicating a good fit between the transmittance data and the calculated curve.

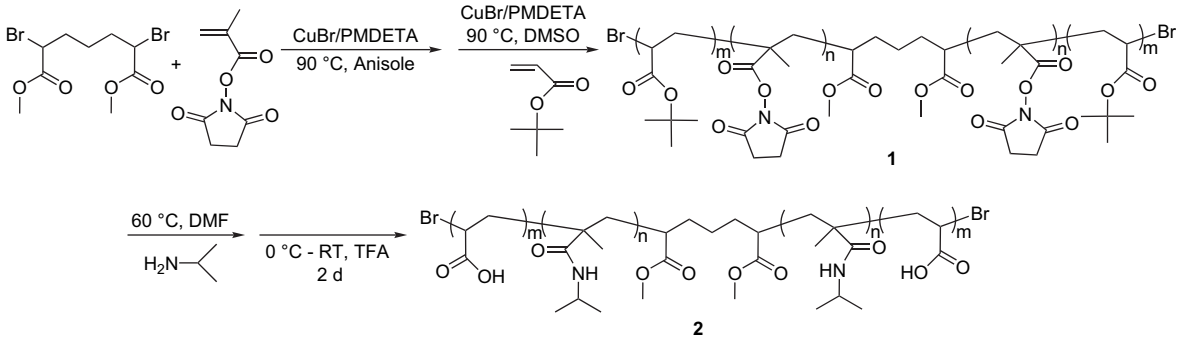

Scheme 3. Synthesis of PAA-*b*-PNIPMAM-*b*-PAA (**2**) triblock copolymer.

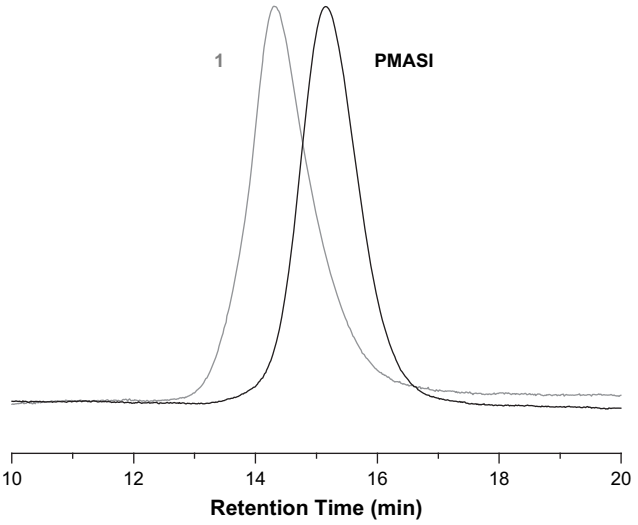

Fig. 3. Overlaid GPC (0.05 M LiBr in DMF, 1 mL/min) traces of PMASI (black) ($M_n = 6.8$ kDa, PDI = 1.16) and P*t*BA-*b*-PMASI-*b*-P*t*BA (**1**, gray) ($M_n = 14.5$ kDa, PDI = 1.24).

The measurements of polymer sample turbidity, with respect to the temperature transition, were reproducible. Three separately prepared solution samples of the same polymer ($M_n = 3.6–6.7$ kDa) produced similar turbidity curves with minor deviation of the cloud point value, $T_{50\%}$ (Table 2). An example is shown in Fig. 5A (blue curve) for the 6.7 kDa PNIPMAM polymer. The higher M_n polymer samples ($M_n = 8.8$ and 9.1 kDa) were difficult to dissolve in solution, requiring long periods of sonication frequently degrading the samples, thus consistent data were difficult to obtain and only one data point is reported. The return transition of the solutions from cloudy to clear occurred between 12 and 24 h. Further research is necessary to determine if this large hysteresis could be utilized for "smart" materials application. The cloud points of a series of the PNIPMAM polymers, as well as PNIPMAM-*b*-PAA diblock and PAA-*b*-PNIPMAM-*b*-PAA (**2**) triblock copolymers, were determined from the turbidity experiments which are outlined in Fig. 5 and summarized in Table 2. The standard deviations of the $T_{50\%}$ values were small for the PNIPMAM polymer series.

The cloud point of LCST capable polymer solutions have been reported to be dependent on the polymers' physical properties such as concentration [20–22] and MW [2,21,22,25–34]. The cloud point data from the turbidity experiments, shown in Fig. 5, were plotted as a function of MW and polydispersity to better understand how these properties relate to the cloud point temperature (Fig. 6). Dashed lines are included in these plots as a visual guide for the trends. The cloud point increases slightly as MW increases (Fig. 6a); however, recent literature has shown a consensus that the cloud point has an inverse dependence on MW, thus the cloud point decreases as MW increases for polymers with low polydispersity [21,22,25–30,32,34]. This disparity in trends could stem from the MW of the PNIPMAM series being determined from calculations based on the GPC data of the PMASI homopolymers. The PMMA standards and PMASI vary in hydrodynamic radius, thus the calculated M_n values from GPC for the PMASI homopolymers are approximate. The disparity in the cloud point trend for MW could also be affected by the

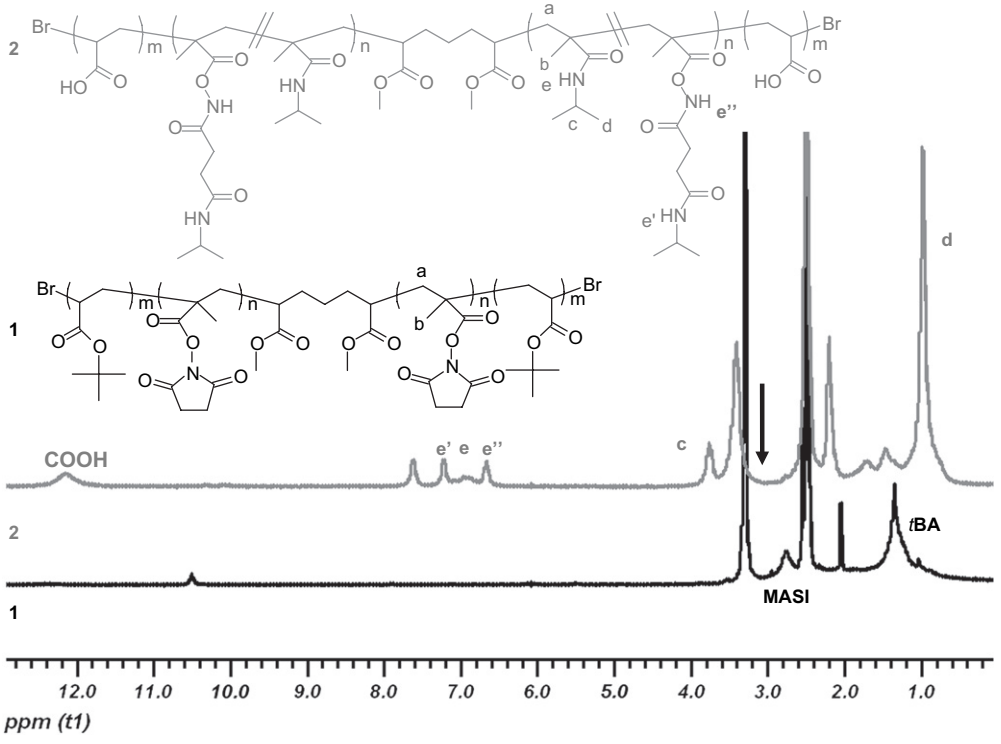

Fig. 4. ^{1}H NMR (DMSO-d_6) comparing P*t*BA-*b*-PMASI-*b*-P*t*BA (**1**, black) with PAA-*b*-PNIPMAM-*b*-PAA (**2**, gray).

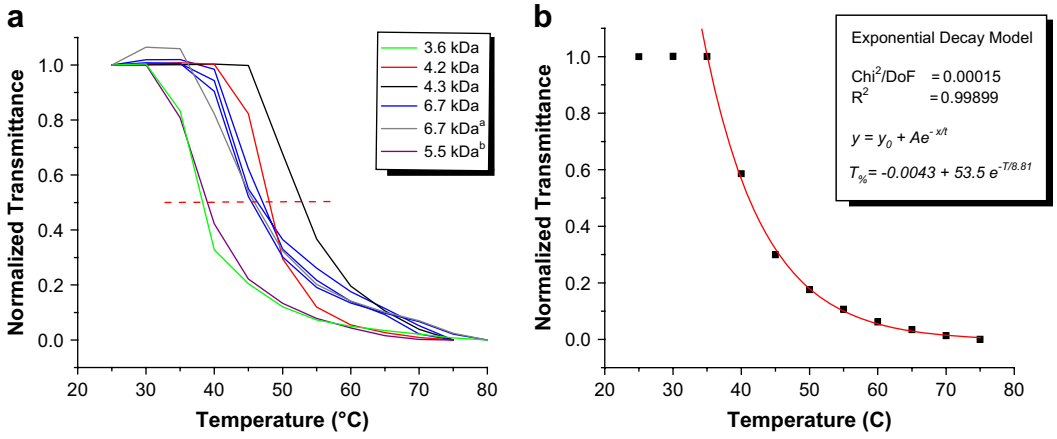

Fig. 5. (a) Cloud point measurements for the PNIPMAM polymers, diblock PNIPMAM-*b*-PAA and triblock PAA-*b*-PNIPMAM-*b*-PAA (**2**) copolymers. Data with the same color (blue) represent multiple trials of the same polymer sample. (b) Exponential fit of turbidity data for calculation of $T_{50\%}$ (3.6 kDa). Calculated M_n for PNIPMAM block of (a) PNIPMAM-*b*-PAA and (b) PAA-*b*-PNIPMAM-*b*-PAA. (For interpretation of the references to colour in this figure legend, the reader is referred to the web version of this article.)

presence of the ring-opened side product, the side product behaving differently in solution from the isopropylamide side group. The ring-opened side product is apparent in all samples, making the role of the side product on changes in the cloud point difficult to elucidate. Further studies are needed with samples of varied side product composition to understand the influence of the side product on the cloud point. However, the apparent M_n of the polymers in solution is also affected by the polydispersity of the polymer. As shown in Fig. 6b, the cloud points decrease with increasing PDI. Due to the relatively low MW ranges of the PNIPMAM series studied here, a broader PDI gives rise to a larger contribution from higher MW polymer chains, thus the cloud point temperature is reduced. This effect of PDI on cloud point is exaggerated for low MW samples and is likely to greatly alter the M_n versus cloud point trend shown in Fig. 6a, for the relatively low M_n series.

The cloud point values for the diblock and triblock copolymers were both lower than the cloud point values for the PNIPMAM polymers having similar PNIPMAM molecular weight. Furthermore, the PNIPMAM blocks in the diblock and triblock copolymers have similar MW, yet the cloud point value of the triblock copolymer is much lower than the diblock copolymer cloud point (38.8 and 45.6 °C, respectively). Determining the effect of PAA content in the block copolymers on the cloud point is difficult due to the many molecular parameters that effect the LCST transition such as composition of the block copolymers and their structure. However, these results suggest that PAA is responsible for making aggregation of the block copolymers more favorable, thus reducing the temperature of the cloud point transition.

The cloud point of LCST polymer solutions has been reported to be pH sensitive as well [18,55,56]. All of the PNIPMAM polymer as well as diblock and triblock copolymer solution samples showed a cloud point transition upon going from a neutral solution (Milli-Q purified water pH = 5.4) to an acidic solution with addition of HCl. This transition was reversible and reproducible many times. The solutions returned to a soluble and clear phase upon going to basic conditions with addition of KOH.

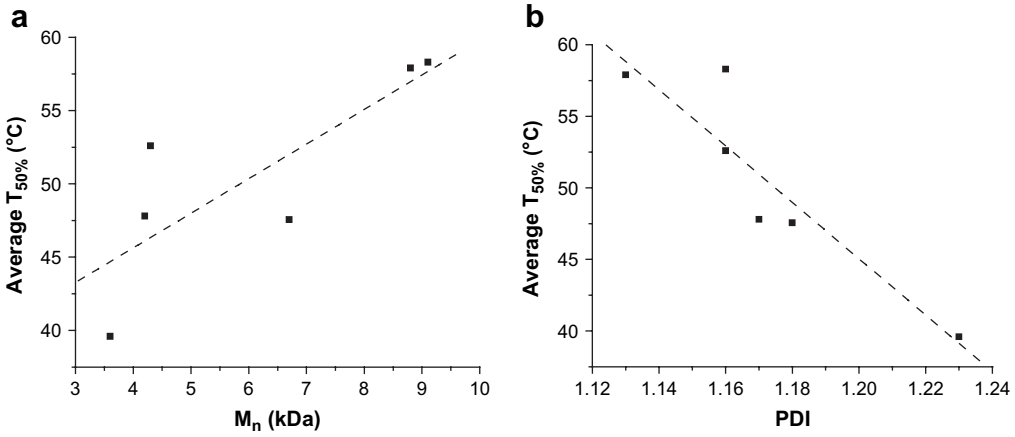

Fig. 6. Average cloud point ($T_{50\%}$) versus (a) M_n and (b) PDI for the PNIPMAM polymer series. Dashed lines shown only for visual guides.

5. Conclusions

PNIPMAM and PNIPMAM block copolymers were synthesized using a post-functionalization approach with relatively narrow polydispersities. A series of PMASI homopolymers were synthesized and functionalized to PNIPMAM, although an upper MW limit was observed due to solubility. The aqueous solution properties of the series were studied and the PNIPMAM polymers were shown to have an LCST phase transition through turbidity measurements. The cloud point transition of the PNIPMAM polymer series is shown to be weakly correlated to MW and has an inverse dependence on polydispersity. The correlation between cloud point and MW was difficult to determine due to the narrow and relatively low MW of the PNIPMAM polymer samples. The ability to synthesize well-defined block copolymers that are thermoresponsive and water-soluble will be of benefit for future applications in drug delivery, bioengineering, and nanotechnology. Although PMASI is shown here with a side reaction (ring-opened amide), our previous work and that from Putnam shows how to avoid these by-products. Also, we recently reported PNSVB which is a styrene based activated ester that showed no side products. These approaches will continue to make post-functionalization a reasonable method for complex architectures and monomers which are difficult to polymerize.

Acknowledgments

The authors thank the Presidential Early Career Awards for Scientists and Engineers (PECASE) and the Army Research Office for the Young Investigator Award and their generous support for this work.

References

[1] Djokpe E, Vogt W. Macromol Chem Phys 2001;202:750–7.
[2] Fujishige S, Kubota K, Ando I. J Phys Chem 1989;93:3311–3.
[3] Chen G, Hoffman AS. Nature 1995;373:49–52.
[4] Hay DNT, Ricket PG, Seifert S, Firestone MA. J Am Chem Soc 2004;126:2290–1.
[5] Hoffmann AS, Stayton PS. Macromol Symp 2004;207:139–51.
[6] Ito T, Hioki T, Yamaguchi T, Shinbo T, Nakao S, Kimura S. J Am Chem Soc 2002;124:7840–6.
[7] Li C, Gunari N, Fischer K, Janshoff A, Schmidt M. Angew Chem Int Ed 2004;43:1101–4.
[8] Pennadam SS, Lavigne MD, Dutta CF, Firman K, Mernagh D, Gorecki DC, et al. J Am Chem Soc 2004;216:13208–9.
[9] Stayton PS, Shimoboji T, Long C, Chilkoti A, Ghen G, Harris JM, et al. Nature 1995;378:472–4.
[10] Sun T, Liu H, Song W, Wang X, Jiang L, Li L, et al. Angew Chem Int Ed 2004;43:4663–6.
[11] Umeno D, Mori T, Maeda M. Chem Commun 1998:1433–4.
[12] Zhu M-Q, Wang L-Q, Exarhos GJ, Li ADQ. J Am Chem Soc 2004;126:2656–7.
[13] Dube D, Francis M, Leroux JC, Winnik FM. Bioconjugate Chem 2002;13:685–92.
[14] Eeckman F, Moes AJ, Amighi K. Eur Polym J 2004;40:873–81.
[15] Eeckman F, Moes AJ, Amighi K. Int J Pharm 2004;273:109–19.
[16] Yamazaki A, Winnik FM, Cornelius RM, Brash JL. Biochim Biophys Acta Biomembr 1999;1421:103–15.
[17] Cui Y, Tao C, Zheng SP, He Q, Ai SF, Li JB. Macromol Rapid Commun 2005;26:1552–6.
[18] Xia Y, Yin XC, Burke NAD, Stover HDH. Macromolecules 2005; 38:5937–43.
[19] Xia Y, Burke NAD, Stover HDH. Macromolecules 2006;39:2275–83.
[20] Heskins M, Guillet JE. J Macromol Sci Chem 1968;A2:1441–55.
[21] Tong Z, Zeng F, Zheng X, Sato T. Macromolecules 1999;32:4488–90.
[22] Zheng X, Tong Z, Xie XL, Zeng F. Polym J 1998;30:284–8.
[23] Duan Q, Miura Y, Narumi A, Shen X, Sato S, Satoh T, et al. J Polym Sci Part A Polym Chem 2006;44:1117–24.
[24] Furyk S, Zhang YJ, Ortiz-Acosta D, Cremer PS, Bergbreiter DE. J Polym Sci Part A Polym Chem 2006;44:1492–501.
[25] Aoshima S, Oda H, Kobayashi E. J Polym Sci Part A Polym Chem 1992;30:2407–13.
[26] Butun V, Armes SP, Billingham NC. Polymer 2001;42:5993–6008.
[27] Kunugi S, Tada T, Tanaka N, Yamamoto K, Akashi M. Polym J 2002; 34:383–8.
[28] Laukkanen A, Valtola L, Winnik FM, Tenhu H. Macromolecules 2004;37:2268–74.
[29] Lessard DG, Ousalem M, Zhu XX. Can J Chem 2001;79:1870–4.
[30] Liu QQ, Yu ZQ, Ni PH. Colloid Polym Sci 2004;282:387–93.
[31] Otake K, Inomata H, Konno M, Saito S. Macromolecules 1990;23: 283–9.
[32] Schild HG, Tirrell DA. J Phys Chem 1990;94:4352–6.
[33] Tiktopulo EI, Uversky VN, Lushchik VB, Klenin SI, Bychkova VE, Ptitsyn OB. Macromolecules 1995;28:7519–24.
[34] Xue W, Huglin MB, Jones TGJ. Macromol Chem Phys 2003;204: 1956–65.
[35] Masci G, Giacomelli L, Crescenzi V. Macromol Rapid Commun 2004;25:559–64.
[36] Neugebauer D, Matyjaszewski K. Macromolecules 2003;36:2598–603.
[37] Rademacher JT, Baum R, Pallack ME, Brittain WJ, Simonsick WJ. Macromolecules 2000;33:284–8.
[38] Teodorescu M, Matyjaszewski K. Macromolecules 1999;32:4826–31.
[39] Teodorescu M, Matyjaszewski K. Macromol Rapid Commun 2000;21:190–4.
[40] Convertine AJ, Ayres N, Scales CW, Lowe AB, McCormick CL. Biomacromolecules 2004;5:1177–80.
[41] Convertine AJ, Lokitz BS, Vasileva Y, Myrick LJ, Scales CW, Lowe AB, et al. Macromolecules 2006;39:1724–30.
[42] Ganachaud F, Monteiro MJ, Gilbert RG, Dourges MA, Thang SH, Rizzardo E. Macromolecules 2000;33:6738–45.
[43] Ray B, Isobe Y, Matsumoto K, Habaue S, Okamoto Y, Kamigaito M, et al. Macromolecules 2004;37:1702–10.
[44] Schilli C, Lanzendorfer MG, Muller AHE. Macromolecules 2002; 35:6819–27.
[45] Hawker CJ, Bosman AW, Harth E. Chem Rev 2001;101:3661–88.
[46] Schulte T, Siegenthaler KO, Luftmann H, Letzel M, Studer A. Macromolecules 2005;38:6833–40.
[47] Monge S, Haddleton DM. Eur Polym J 2004;40:37–45.
[48] Shunmugam R, Tew GN. J Am Chem Soc 2005;127:13567–72.
[49] Shunmugam R, Tew GN. J Polym Sci Part A Polym Chem 2005;43:5831–43.
[50] Wong SY, Putnam D. Bioconjugate Chem 2007;18:970–82.
[51] Aamer KA, Tew GN. J Polym Sci Part A Polym Chem 2007;45: 5618–25.
[52] Alb AM, Enohnyaket P, Drenski MF, Shunmugam R, Tew GN, Reed WF. Macromolecules 2006;39:8283–92.
[53] Aamer KA, Tew GN. J Polym Sci Part A Polym Chem 2007;45: 1109–21.
[54] Aamer KA, Tew GN. Macromolecules 2007;40:2737–44.
[55] Cho EC, Lee J, Cho K. Macromolecules 2003;36:9929–34.
[56] Tanaka T, Fillmore D, Sun ST, Nishio I, Swislow G, Shah A. Phys Rev Lett 1980;45:1636–9.